RAPID COMMUNICATIONS

PHYSICAL REVIEW A VOLUME 44, NUMBER 9 1 NOVEMBER 1991

Suppression of ionization in short high-frequency laser pulses of high intensity

Marko Horbatsch
Physics Department, York University, Toronto, Ontario, Canada M3J 1P3
(Received 13 March 1991)

A numerical technique for the solution of the time-dependent Schrödinger equation in three spatial dimensions is proposed to study the time evolution of hydrogen atoms subject to ultraintense short laser pulses. The method makes use of the Kramers-Henneberger transformation, and through a variable substitution, all of position space is discretized and the correct boundary condition at infinity is implemented. Calculations for 6-fs pulses with a $\sin^2$-shaped envelope show that stabilization of the atom against ionization does occur at high laser frequency and intensity, but that it is much less efficient than predicted by one-dimensional model calculations.

PACS number(s): 32.80.Rm, 42.50.Hz

The study of even simple atoms like hydrogen in very intense laser fields has recently become an area of considerable theoretical interest [1]. Large-scale numerical calculations that deal with this problem include Floquet theory [2,3] (for monochromatic fields), direct integration of the time-dependent Schrödinger equation (TDSE) by various methods [4–6], and treatment of many-electron atoms by TD mean-field theory [7,8]. Very elaborate numerical calculations exist within the framework of a one-dimensional (1D) model [9–13], which resembles the 3D problem in that the eigenvalue spectrum contains both a Rydberg series and a continuum.

A remarkable theoretical result has been obtained by transforming the TDSE into a frame that follows the oscillatory motion, which a classical particle experiences, if it is exposed to the laser field alone. In this Kramers-Henneberger (KH) frame one can derive the result that ionization is inhibited for monochromatic intense laser fields of high frequency [14]. However, it is not evident that this stability against ionization persists, if the laser field is switched on by an envelope function (as happens in experiments). The idea that such a stabilization indeed occurs, even for short pulses with a realistic envelope, received support from 1D model calculations [9–13]. These calculations, performed on rather large spatial meshes suggest that in the presence of a strong high-frequency laser field, while the ground state is depopulated, the Rydberg levels play an important role and the population of these states prevents ionization. Furthermore, it follows in this model that for field strengths of the order of several atomic units (a.u.), about 30%–50% of the electronic probability distribution oscillates between two turning points or remains trapped near the nucleus and cannot ionize.

A very recent semiclassical investigation suggests that in the 3D case stabilization of atoms should be less important than predicted by the 1D model [15]. According to this analysis, which relies on propagating a microcanonical ensemble of test particles that follow classical trajectories, stabilization is prevented by the amount of phase space that the additional degrees of freedom have to offer for ionizing trajectories. Another, relatively small, destabilizing contribution comes from the inclusion of relativistic dynamics. The aim of this contribution is to clarify this matter by presenting results from numerical solutions of the TDSE in 3D.

The TDSE in the laboratory frame in atomic units for a linearly polarized laser field reads as

$$i\frac{\partial}{\partial t}\psi(\mathbf{r},t)=\left[-\frac{1}{2}\nabla^2-\frac{Z}{r}-E_x(t)x\right]\psi(\mathbf{r},t)\,. \qquad (1)$$

For monochromatic fields the transformation to a Floquet representation turns out to be convenient [2,3], but in order to study effects of the switching of the laser pulse one has to integrate Eq. (1) directly. The pulse shape used in this work is of the form $E_x(t)=E_0\sin(\omega t)\times\sin^2(\pi t/T)$. Here ω is the laser frequency, E_0 the peak strength of the laser field, and T the length of the pulse.

Kulander's work [4,7] relies on a finite difference approximation of Eq. (1). It follows ideas laid out for 1D problems in Ref. [16] and extends these to the 3D case with cylindrical symmetry. The numerical solution of Eq. (1) using a mesh with constant spacing in the cylindrical (ρ,z) coordinates requires the incorporation of boundary conditions at a finite distance in coordinate space. In order to avoid a reflection of the ionizing part of the electronic charge distribution back into the vicinity of the atomic nucleus one has to apply an imaginary potential on the surface of the mesh. The strength of this potential has to be chosen carefully in order not to affect the physical results. Another problem concerns the accuracy of such calculations as a function of the mesh spacings $\Delta\rho$ and Δz. The energy-momentum dispersion relation for free particles will be satisfied accurately only for momenta up to the order of $1/\Delta x$. For strong external fields one also has to worry about the dispersion relation in those regions of space, where the potential is large [16]. From numerical experiments, based on a discretization of Eq. (1) for the propagation of wave packets under the influence of a constant force field, we conclude that for field strengths of the order of 1 a.u. calculations with a spacing of $\Delta x=0.1$ a.u. become unreliable after $t\approx 10$ a.u. due to this effect.

A resolution to this problem is given by transforming Eq. (1) into the KH frame [12]. The TDSE transforms under this translation by a gauge transformation, i.e., both

the Hamiltonian and the wave function are being transformed. The TDSE in this frame becomes [12]

$$i\frac{\partial}{\partial t}\phi(\mathbf{r},t)=\left[-\frac{1}{2}\nabla^2-\frac{Z}{|\mathbf{r}+\boldsymbol{\alpha}(t)|}\right]\phi(\mathbf{r},t)\,, \qquad (2)$$

where the displacement $\boldsymbol{\alpha}(t)$ is given as the integral of the classical equation of motion in the force field $E_x(t)$. Extraction of the probabilities to remain in the ground state or to inclusively occupy bound states is possible in the same way as in the laboratory frame. Within each cycle there are two points in time at which the displacement $\boldsymbol{\alpha}(t)$ vanishes and the projections onto basis states are identical in both frames up to an irrelevant phase factor. For photoelectron spectra one even has the advantage that the results in the KH frame are free of the ponderomotive shifts.

Before the discretization of Eq. (2) the position variables (x,y,z) are mapped onto a finite interval using the transformation $r_i=\beta_i\tan\theta_i$. This substitution renders the TDSE amenable to an explicit time integration and allows one to incorporate the boundary condition that the wave function vanishes at infinity [17]. The scale parameters β_i can be adjusted so that an equidistant mesh in θ_i covers an appropriate region in r_i space. The problem is discretized in Cartesian coordinates, as future investigations will focus on circularly polarized light and the inclusion of magnetic-field effects.

The numerical solution of the transformed TDSE proceeds by the Crank-Nicholson method. The meshes used were of size $64\times48\times48$ for (x,y,z) space and values for the β_i were tried in the range between 5 and 10 a.u. The equidistant mesh in the θ_i variables results in a nonuniform mesh for the Cartesian coordinates. Thorough testing was performed on the mesh size and the value of the scale parameters in the transformation in order to work in a stable regime of parameters and results from other methods in the literature [3,4,8] were reproduced. The initial H(1s) wave function was generated on the mesh using an iterative technique to solve large-scale eigenvalue problems for the ground state. Probabilities for the occupation of the initial state as well as the probability to remain in a volume of size 10 a.u. (to be interpreted as an inclusive bound-state occupation probability) were calculated. They allow one to estimate the total ionization probability as well as the ionization rate in the regime where the time evolution of the ionization probability is nearly exponential.

Figure 1 shows the time evolution of the position expectation value as calculated in the KH frame and then translated into the laboratory frame for a 6-fs pulse with a wavelength of 92 nm and a peak intensity of 1.4×10^{17} W/cm^2. It can be seen that in the KH frame the electronic wave function undergoes much less motion than in the laboratory frame and thus there is much less danger to loose accuracy due to the discretization of the kinetic-energy operator. Particularly interesting is the observation that the position expectation value in this frame stabilizes after some initial oscillations. The initial oscillations are caused by the binding of the electronic wave function to the nucleus. Position expectations for $x>0$ and $x<0$ separately in the KH frame are larger in magnitude than the sum shown in Fig. 1, but still very small compared to the laboratory-frame result.

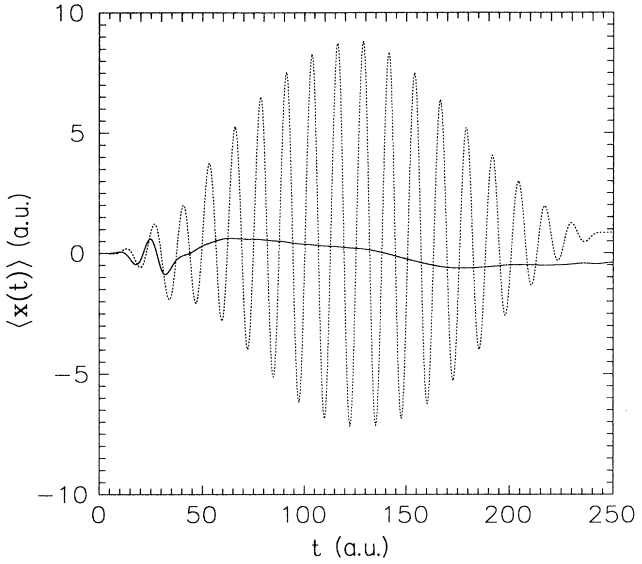

FIG. 1. Position expectation value $\langle x(t)\rangle$ for a 6-fs laser pulse with field strength $E_0=2$ a.u. and frequency $\omega=0.5$ a.u. Dashed line: laboratory frame; solid line: KH frame.

Figure 2(a) shows the time evolution of the probability to remain in the ground state as well as of the probability to remain within a sphere or radius 10 a.u. for a peak field intensity of 3.6×10^{14} W/cm^2. The complement of the inclusive bound-state occupation probability to unity is interpreted as the total ionization probability. It can be seen that the time evolution of both the 1s and inclusive bound-state decay probabilities is parallel in the regime of exponential decay. For higher frequencies and peak intensities they are no longer parallel. Given the shape of the pulse, which can be visualized from the average displacement shown in Fig. 1, one can notice the following: depopulation of the ground state and ionization sets in after the field has reached some critical value; at this critical-field strength the wave function can escape over the potential barrier that forms as a result of adding the Coulomb potential and the linear potential from the laser field. The critical value is lower than the one found in Ref. [12], since the 1D model binds the electron too strongly. It is interesting to observe that a regime with a single exponential decay constant prevails after the field has passed through its peak. Even for this moderate intensity the decay constant approaches its value before the peak has been reached.

In Fig. 2(b) results are shown for the case of a peak intensity of 1.4×10^{17} W/cm^2. Due to the significantly higher field strength the ground-state depopulation and ionization processes begin to occur in the early stages of the laser pulse. An exponential decay regime can be observed for times in the vicinity of $t=50$ a.u., but saturation sets in as the ionization probability reaches 90%. The H (1s) occupation probability and subsequently also the inclusive bound-state probability develop an irregular behavior as a function of time. The deviation from exponen-

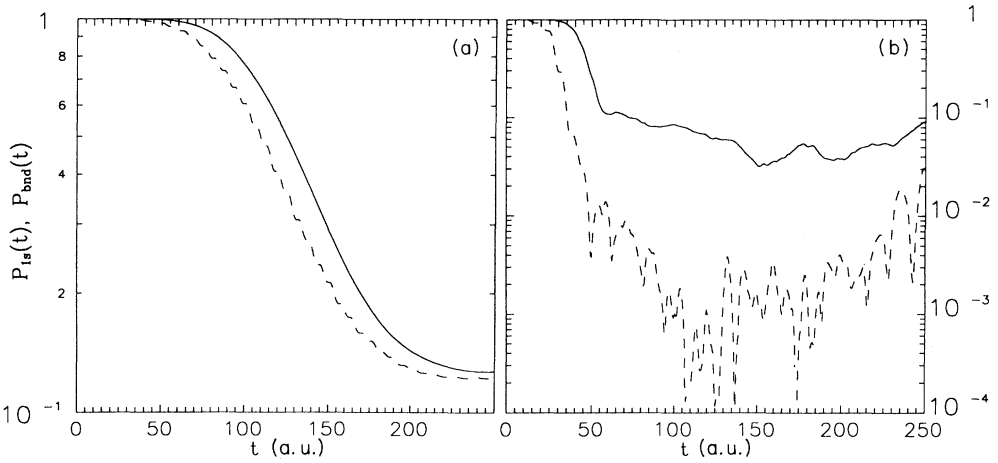

FIG. 2. Time evolution of the inclusive bound-state probability (solid line) and the H ($1s$) probability (dashed line) for a 6-fs laser pulse with frequency $\omega=0.5$ a.u. and peak field (a) $E_0=0.1$ a.u. and (b) $E_0=2$ a.u.

tial decay and the saturation of the ionization rate, which appear after $t=60$ a.u., are caused by the presence of the strong laser field. After the passage of the strong peak field values no further ionization is observed. On the contrary, the occupation of bound states, including the ground state, picks up towards the end of the laser pulse.

In order to study the systematic dependence of the efficiency to ionize for laser pulses of a given shape and wavelength, but varying in peak field strength, we have extracted two quantities. The average total ionization probability was obtained by averaging the ionization probability over the final quarter of the pulse. The average ionization rate was extracted from the region in time where the decay follows exponential behavior. This part includes a range of ionization probability, where at least 60% of the atom decays for all strong-field cases considered.

These quantities are shown in Fig. 3 as a function of peak field strength. For $\omega=0.5$ a.u. and peak fields below 0.1 a.u. a strong rise of the ionization rate as a function of intensity is apparent. Due to the finite duration of the pulse the average ionization probability after the pulse remains above 10% in this regime. As the peak strength increases towards 1 a.u. a saturation in the rate can be observed at a value which is a factor of 2 below the peak ionization rate observed for monochromatic laser fields. Here the depopulation of bound states reaches a maximum of 99%. As the peak field strength is increased further, the average ionization rate stays constant in contrast to the monochromatic field calculations. The strong-field stabilization phenomenon is, however, responsible for reducing the average total ionization probability to only 90%. This latter value of the average ionization probability is in contrast with the 1D model calculations, where final values of only 50% were found [10,11]. It is, however, consistent with recent findings within a semiclassical calculation [15], which compares results in one and three dimensions. This calculation also indicates that relativistic as well as magnetic-field effects begin to play a small role at the end of higher peak field strengths shown in Fig. 3.

To study the dependence of the high-field stabilization phenomenon on the laser frequency calculations were performed with $\omega=0.75$ and 1 a.u. and the same number of 20 cycles of the laser field. The ionization rate grows less rapidly as a function of peak field strength and the maximum average ionization probability amounts to 96%. These changes are too large in order to be caused by the shortening of the laser pulse alone. They show that ionization is inhibited to some degree at higher frequencies. It follows that one has to go to much higher frequencies than suggested by monochromatic and 1D model calculations in order to observe significant stabilization in strong fields. Calculations with $\omega=1$ a.u. show similar behavior to the ones for $\omega=0.75$ a.u., except that for strong fields

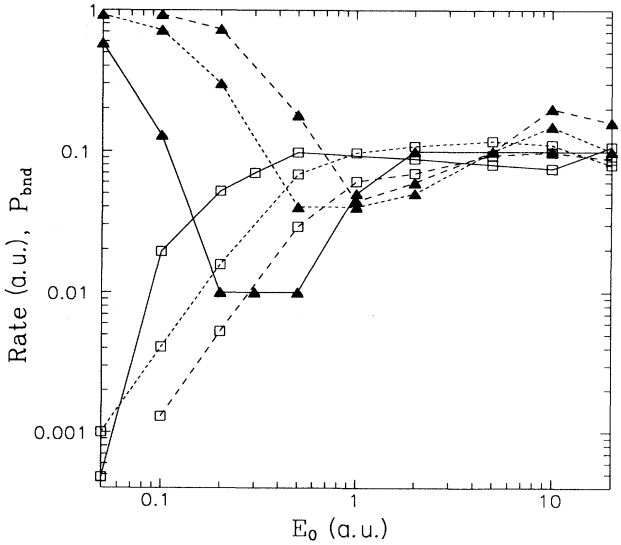

FIG. 3. Average ionization rate (squares, see text) and inclusive bound-state probability (triangles) as a function of maximum field strength E_0 for 6-fs laser pulses of frequency $\omega=0.5$ a.u. (solid lines), $\omega=0.75$ a.u. (short-dashed lines), and $\omega=1.0$ a.u. (dashed lines).

two exponential decay regimes appear. This is somewhat indicated already in Fig. 2(b). For higher frequencies the rapid decay regime includes only the decay of about 50% of the atom and a second exponential regime with a decay constant smaller by about an order of magnitude follows. For strong fields ($E_0 > 1$ a.u.) final ionization probabilities of only 80% are found. These values are significantly lower than the semiclassical results for the same frequency [15], but somewhat different pulse shape.

We also performed variations of the pulse length. For $\omega = 0.5$ a.u. and $T = 12$ fs the following observations are made: for weaker fields (below $E_0 = 0.2$ a.u.) the decay rate is the same and the total ionization probability increases due to the longer time exposure. For intermediate peak strength $E_0 = 0.5$–1.0 a.u. a lowering of the ionization rate by up to a factor of 2 is found, which shows that for large enough T stabilization does occur.

In conclusion, 3D calculations show that for pulses of short duration, such as 6 fs, it is possible to define an average ionization rate and a total ionization probability. The total ionization probabilities for short pulses are much larger than those obtained from calculations within a 1D model potential. Saturation behavior of the average ionization rates at high peak field strength is found, which disagrees with the monochromatic field result [3], where the ionization rate has a maximum at a field of 1 a.u. and then falls for stronger fields. Significantly reduced ionization probabilities (of the order of 80% only) are found for 20-cycle pulses with $\omega = 1$ a.u. The inclusion of magnetic-field effects or the treatment of circular and elliptical laser polarization does not represent any additional technical problems in the present method. Future work will include an analysis of the energy distribution of the emitted electrons.

I thank Ken Kulander for discussions. The financial support of the Natural Sciences and Engineering Research Council of Canada is gratefully acknowledged.

[1] J. Opt. Soc. Am. B **7**, 403–688 (1990).
[2] S.-I. Chu and J. Cooper, Phys. Rev. A **32**, 2769 (1985).
[3] M. Dörr, R. M. Potvliege, and R. Shakeshaft, Phys. Rev. Lett. **64**, 2003 (1990).
[4] K. C. Kulander, Phys. Rev. A **35**, 445 (1987).
[5] P. L. De Vries, J. Opt. Soc. Am. B **7**, 517 (1990).
[6] X. Tang, H. Rudolph, and P. Lambropoulos, Phys. Rev. Lett. **65**, 3269 (1990).
[7] K. C. Kulander, Phys. Rev. A **36**, 2726 (1987).
[8] M. S. Pindzola, G. J. Bottrell, and C. Bottcher, J. Opt. Soc. Am. B **7**, 659 (1990).
[9] J. Javanainen, J. H. Eberly, and Q. Su, Phys. Rev. A **38**, 3430 (1988).
[10] Q. Su, J. H. Eberly, and J. Javanainen, Phys. Rev. Lett. **64**, 862 (1990).
[11] Q. Su and J. H. Eberly, J. Opt. Soc. Am. B **7**, 564 (1990).
[12] V. C. Reed and K. Burnett, Phys. Rev. A **42**, 3152 (1990).
[13] K. Burnett, P. L. Knight, B. R. M. Piraux, and V. C. Reed, Phys. Rev. Lett. **66**, 301 (1991).
[14] M. Pont and M. Gavrila, Phys. Rev. Lett. **65**, 2362 (1990), and references therein.
[15] J. Grochmalicki, M. Lewenstein, and K. Rzążewski, Phys. Rev. Lett. **66**, 1038 (1991).
[16] A. Goldberg, H. M. Schey, and J. L. Schwartz, Am. J. Phys. **35**, 177 (1967).
[17] M. Horbatsch, J. Phys. B **17**, 2591 (1984).